PHYSICS OF FLUIDS **26**, 106601 (2014)

The mean flow and long waves induced by two-dimensional internal gravity wavepackets

T. S. van den Bremer[1,a)] and B. R. Sutherland[2,3,b)]
[1]*Department of Engineering Science, University of Oxford, Parks Road, Oxford OX1 3PJ, United Kingdom*
[2]*Department of Physics, University of Alberta, Edmonton, Alberta T6G 2E1, Canada*
[3]*Department of Earth and Atmospheric Sciences, University of Alberta, Edmonton, Alberta T6G 2E3, Canada*

(Received 30 July 2014; accepted 13 October 2014; published online 28 October 2014)

Through theory supported by numerical simulations, we examine the induced local and long range response flows resulting from the momentum flux divergence associated with with a two-dimensional Boussinesq internal gravity wavepacket in a uniformly stratified ambient. Our theoretical approach performs a perturbation analysis that takes advantage of the separation of scales between waves and the amplitude envelope of a quasi-monochromatic wavepacket. We first illustrate our approach by applying it to the well-studied case of deep water surface gravity waves, showing that the induced flow, $U_{\rm DF}$, resulting from the divergence of the horizontal momentum flux is equal to the Stokes drift. For a localized surface wavepacket, $U_{\rm DF}$ is itself a divergent flow and so there is the well-known non-local response manifest in the form of a deep return flow beneath the wavepacket. For horizontally periodic and vertically localized internal wavepackets, the divergent-flux induced flow, $u_{\rm DF}$, is found from consideration of the vertical gradient of the vertical flux of horizontal momentum associated with the waves. Because $u_{\rm DF}$ is itself a non-divergent flow field, this accounts entirely for the wave-induced flow; there is no response flow. Our focus is upon internal wavepackets that are localized in the horizontal and vertical. We derive a formula for the divergent-flux induced flow that, as in this case of surface wavepackets, is itself a divergent flow. We show that the response is a horizontally long internal wave that translates vertically with the wavepacket at its group velocity. Scaling relationships are used to estimate the wavenumber, horizontal extent, and amplitude of this induced long wave. At higher order in perturbation theory we derive an explicit integral formula for the induced long wave. Thus, we provide validation of Bretherton's analysis of flows induced by two-dimensional internal wavepackets [F. P. Bretherton, "On the mean motion induced by gravity waves," J. Fluid Mech. **36**, 785–803 (1969)] and we provide further analyses that give intuitive insights into the physics governing the properties of the induced long wave. In particular, consistent with momentum conservation, we show that the horizontally-integrated horizontal flow associated with the long wave is given exactly by the horizontal integral of $u_{\rm DF}$. However, qualitatively different from horizontally periodic internal waves, the vertical profile of the induced horizontal flow across the horizontally localized wavepacket is positive at the leading edge and negative at the trailing edge. These results are validated by the results of numerical simulations of a Gaussian wavepacket initialized in an otherwise stationary ambient. © *2014 AIP Publishing LLC*. [http://dx.doi.org/10.1063/1.4899262]

a)Email: ton.vandenbremer@eng.ox.ac.uk
b)Email: bruce.sutherland@ualberta.ca. URL: http://www.ualberta.ca/~bsuther.

I. INTRODUCTION

Internal waves propagate vertically through the atmosphere and ocean moving under the influence of buoyancy forces in a stratified medium. Where they break, the consequent momentum-flux divergence irreversibly accelerates the ambient fluid. Cumulatively in the atmosphere, this non-negligibly affects the zonal wind speeds and, through thermal wind balance, the mean temperatures.[2–4] Despite their importance, the mechanism for momentum transport and deposition by internal waves remains unclear. Although linear theory is sometimes employed to predict where anelastic internal waves break,[5] it is now clear that weakly nonlinear effects can significantly change the evolution and breaking levels.[6–8] Most studies into vertically propagating weakly nonlinear internal waves have examined wavepackets that are vertically localized and horizontally periodic. Such wavepackets have a well-defined wave-induced mean flow that translates vertically with the wavepacket at its group velocity before being irreversibly deposited to the background when the waves break. Even before breaking, the wave-induced mean flow Doppler shifts the waves as they grow to large amplitude giving rise to modulational stability or instability.[6] If an internal wavepacket is horizontally as well as vertically localized, the direct counterpart to the induced flow for horizontally periodic waves is a horizontally divergent flow field. And so there must be response flow that ensures the total flow field is incompressible. Using the concept of wave-action conservation, Bretherton[1] examined the wave-induced flow resulting from two- and three-dimensional internal wavepackets. He predicted that a small-amplitude localized two-dimensional wavepacket should excite a horizontally long disturbance while a three-dimensional (spanwise localized) wavepacket should generate a horizontal recirculation, which in itself could have a far-field influence on the ambient.[9,10]

In this paper we revisit the theory for the flow induced by two-dimensional internal wavepackets. Our objectives are threefold. First, rather than relying on wave-action conservation, we develop a wavepacket-based theory to derive intuitive formulae for the (local) divergent-flux induced flow and the (non-local) induced long wave associated with a localized quasi-monochromatic wavepacket. Second, we derive approximate scaling estimates and analyses of the integral equation describing the induced long wave that provides insight into the structure of the non-local motion induced by the wavepacket. Third, we compare the theoretical predictions with fully nonlinear numerical simulations of a small-amplitude wavepacket initialized in a stationary ambient. Thus we observe the approach to steady-state and confirm that this is consistent with the theoretical predictions. These results provide the foundation for theoretical and physical understanding upon which future studies into large-amplitude and three dimensional effects will be developed further.

To lay the theoretical groundwork, we first review the theory for the wave-induced flow of surface wavepackets and of horizontally periodic, vertically localized internal wavepackets.

Even without breaking, surface gravity waves have associated with them a wave-induced flow known commonly as the Stokes drift.[11] From a Lagrangian perspective, the flow is a consequence of fluid parcels being advected further in the wave-direction at the top of their orbits than they propagate in the opposite direction at the bottom of their orbits, as well as an equivalent effect during motion in the horizontal direction. The expression for the vertical integral of the Stokes drift is equal to the pseudomomentum per unit mass. But the latter is conceptually distinct, arising from consideration of conservation laws. The formulae for the Stokes drift and pseudomomentum have been derived for plane waves, but are readily extended to wavepackets. In Sec. II A, we present another perspective, showing that the pseudomomentum per unit mass is identical to the flow arising from the divergence of the horizontal flux of horizontal momentum associated with a quasi-monochromatic wavepacket. This we refer to as the "divergent-flux induced flow." If the surface wavepacket has finite horizontal extent, the Stokes drift is zero ahead and behind the wavepacket resulting in a convergence and divergence of the horizontal flow at the wavepacket's leading and trailing edge, respectively. This results in a response flow that moves opposite to the direction of the Stokes drift, and is hence referred to as the return flow. For deep water it extends far below the surface[12] (cf. Fig. 2 of McIntyre[13]). The vertically integrated volume flux of this response flow is equal and opposite to the volume flux associated with the Stokes drift. It is for this reason that the Stokes drift is sometimes referred to

as the *pseudo*momentum per unit mass, a reminder that the actual momentum of the wavepacket (which includes the return flow) is zero.[13]

For internal waves in a uniformly stratified fluid, the properties of their associated wave-induced flow are not so well understood. It is well known that plane periodic Boussinesq internal waves are an exact solution of the fully nonlinear equations of motion. The mean Lagrangian displacement of fluid parcels due to the waves is zero: there is no Stokes drift. However, the pseudomomentum, inferred through wave-action conservation[1,14,15] or derived through the principles of Hamiltonian fluid dynamics,[16] is non-zero.[10] Indeed, for horizontally periodic, vertically localized internal wavepackets, the pseudomomentum per mass gives the wave-induced mean flow.[17] This is a transient, horizontally uniform flow that translates vertically with the wavepacket at the vertical group velocity. Through a separate theoretical approach that examines momentum transport by quasi-monochromatic wavepackets, the origin of the wave-induced mean flow for horizontally periodic wavepackets is clear: the flow results from the vertical divergence of the horizontal momentum flux.[18,19] The derivation of this divergent-flux induced flow is reviewed in Sec. II B.

If a two-dimensional internal wavepacket is horizontally as well as vertically localized, the divergence of the pseudomomentum is non-zero. And so, as in the case of surface wavepackets, there must be a response flow. However, this flow cannot simply return above and below the wavepacket because stratification inhibits vertical motions associated with such a re-circulation. Different from the approach of Bretherton,[1] in Sec. III we use a wavepacket approach to derive what we call the "divergent-flux induced flow" for localized internal wavepackets. Therein we show that the divergent-flux induced flow itself induces a response flow such that the total wave-induced flow extends broadly in the horizontal to either side of the wavepacket. Higher-order perturbation theory reveals that the flow induced by the wavepacket is a horizontally long internal wave that moves vertically with the wavepacket.

In Sec. IV these predictions are compared with numerical simulations a of quasi-monochromatic horizontally periodic and horizontally localized wavepackets showing that the theory well captures the flow induced by a small-amplitude internal wave after a transient start-up time. Conclusions are drawn and implications discussed in Sec. V.

II. SURFACE WAVES AND HORIZONTALLY PERIODIC INTERNAL WAVES

In this section we begin by reviewing the theory for the wave-induced mean flow associated with surface waves. Therein we show that the Stokes drift is equal (but not equivalent) to the pseudomomentum per unit mass and that both are reproduced by consideration of the divergence of the horizontal flux of horizontal momentum associated with quasi-monochromatic surface wavepackets. Likewise we show that the divergence of the vertical transport of horizontal momentum associated with horizontally periodic internal wavepackets reproduces the pseudomomentum. With this physically intuitive derivation of the wave-induced flow which is local to the wavepacket, we go on to examine the divergent-flux induced flow and the total wave-induced flow associated with horizontally and vertically localized wavepackets, which are non-local to the wavepacket.

A. Surface gravity waves

The purpose of this section is not only to review the theory for surface waves, but also to establish the mathematical terminology in a familiar setting. Plane surface gravity waves in deep water of horizontal wavenumber k (assumed positive) have frequency $\omega = \sqrt{gk}$, in which g is gravity and we have assumed $\omega > 0$ corresponding to rightward-propagating waves. Assuming the waves have vertical-displacement amplitude A_0, the polarization relations give the horizontal and vertical velocities:

$$u = \omega A_0 e^{kz} e^{\imath(kx-\omega t)}, \tag{1a}$$

$$w = -\imath\omega A_0 e^{kz} e^{\imath(kx-\omega t)}, \tag{1b}$$

and the corresponding horizontal and vertical displacement fields:

$$\xi_x = \imath A_0 e^{kz} e^{\imath(kx-\omega t)}, \tag{2a}$$

$$\xi_z = A_0 e^{kz} e^{\imath(kx-\omega t)}, \tag{2b}$$

in which it is understood that the actual fields are the real part of the right-hand expressions.

Averaging these fields in time over one period gives zero. However, performing a Taylor-series expansion of the horizontal velocity up to order amplitude squared (thus following particles in their leading-order Lagrangian motion) and averaging gives[11]

$$U_{\mathrm{SD}} = \langle u \rangle + \langle \xi_x \, \partial_x u \rangle + \langle \xi_z \, \partial_z u \rangle = (\omega/k)\alpha^2 e^{2kz} \tag{3}$$

in which $\alpha \equiv A_0 k$ is the wave steepness and $\langle \cdot \rangle$ denotes averaging over either a period or a wavelength. This is the Stokes drift, which corresponds to the mean Lagrangian advection of fluid parcels by a surface wave in the absence of any background (i.e., Eulerian) flow. The corresponding Lagrangian volume flux is given by vertically integrating (3). Multiplied by the density of water ρ_0 the Stokes drift of periodic surface gravity waves has an associated vertically integrated momentum:

$$M = \rho_0 \frac{\omega}{2k^2} \alpha^2. \tag{4}$$

An analogous result was first derived in an Eulerian framework by Starr.[20] In an Eulerian framework, a net mass flux is identified by integrating the horizontal velocity from the bottom up to the free surface. Because the flow is higher at a crest than at a trough, the result gives a mean depth-integrated horizontal flux consistent with the flux obtained by depth integration of (3).

The vertically integrated energy associated these waves is $E = \rho_0 (g/2) {A_0}^2$. The analogy to momentum as a conserved quantity for fluids is the so-called "pseudomomentum," which, from the principle of conservation of wave-action,[14] is given generally for waves in a stationary ambient by

$$P = kE/\omega. \tag{5}$$

Substituting the expression for E into (5) and using the dispersion relation reveals that $P = M$: the pseudomomentum is equal to the momentum computed from the Stokes drift.

These results have assumed an infinitely periodic wave train. Perhaps a more physically intuitive appreciation of the near-surface momentum associated with surface waves comes from consideration of quasi-monochromatic surface wavepackets. By analogy with (1), we suppose the horizontal and vertical velocity fields are given by

$$u^{(1)} = \omega A(X, T) e^{kz} e^{\imath(kx-\omega t)}, \tag{6a}$$

$$w^{(1)} = -\imath \omega A(X, T) e^{kz} e^{\imath(kx-\omega t)}, \tag{6b}$$

in which A is the amplitude envelope with initial magnitude $A_0 \equiv ||A||$, and the superscripts on the left-hand side emphasize that these are velocities given to $O(\alpha^1)$. The amplitude envelope is assumed to vary slowly in space and time compared to the fast scales k^{-1} and ω^{-1}, respectively. The leading-order evolution of the wavepacket is its translation at the group velocity. This is captured by setting $X \equiv \epsilon(x - c_g t)$ with $\epsilon = 1/(\sigma k) \ll 1$, in which σ represents the spatial extent of the wavepacket and $c_g = (\sqrt{g/k})/2$ is the group velocity. The dispersion of the wavepacket is a slower process that depends upon the curvature of the amplitude envelope, as represented by $T = \epsilon^2 t$. Because our examination is not concerned with weakly nonlinear effects, we need not provide a scaling between α and ϵ for the multiple scale asymptotic expansion that follows.

Now consider the flux-form of the horizontal momentum equation:

$$\partial_t u = -\partial_x(uu) - \partial_z(uw) - \partial_x(p/\rho_0). \tag{7}$$

Substituting (6) into the advective terms on the right-hand side and keeping the slowly varying terms we find that the vertical divergence term vanishes because $u^{(1)}$ and $w^{(1)}$ are 90° out of phase. The

remaining flux term is:

$$-\partial_x \overline{u^{(1)}u^{(1)}} \to -\epsilon \partial_X \left[\frac{\omega^2}{2} |A(X,T)|^2 e^{2kz} \right]. \tag{8}$$

Here the over-line denotes effective averaging over the fast scales so as to retain only slowly varying terms. As a result, we have retained the x-derivative term in (8), which represents the horizontal transport of horizontal momentum per unit mass.

The order α^2 divergent flux in (8) results in an acceleration which itself must be order α^2. The resulting divergent-flux induced flow we denote by $U_{\mathrm{DF}}(X,T)$, an $O(\alpha^2)$ quantity that translates at the group velocity of the surface wavepacket. Substituting U_{DF} on the left-hand side of (7) and taking the time derivative gives $-\partial_t U_{\mathrm{DF}} \simeq -\epsilon c_g \partial_X U_{\mathrm{DF}}$, in which we have retained terms of order ϵ alone. Equating this to the divergent-flux term and integrating in X gives the explicit expression for the divergent-flux induced flow:

$$U_{\mathrm{DF}} = \frac{1}{c_g} \overline{u^{(1)}u^{(1)}} = \omega k |A|^2 e^{2kz}. \tag{9}$$

For plane waves $|A| = A_0$ and (9) becomes equal to the formula for the Stokes drift (3). The vertical integral of (9) after multiplying by density gives the pseudomomentum, given by generally (5) and specifically by (4). The physics of the near-surface flow are clear under this macroscopic examination of the momentum conservation law, which reveals that the horizontal flow results from the divergence of the horizontal flux of horizontal momentum per unit mass.

Of course, this is not the whole story. Because U_{DF} for horizontally localized wavepackets is itself a horizontally divergent flow there must also be a response flow in order to ensure volume is conserved. This is taken care of by the pressure gradient term in (7). The divergence of U_{DF} gives rise to an order α^2 pressure $p^{(2)}$ that drives a return flow $\vec{U}_{\mathrm{RF}}$ below the wavepacket. The structure of this flow was first computed by Longuet-Higgins and Stewart[12] (cf. Figure 2 of McIntyre[13]) through a spectral analysis that extracted a mean flow resulting from wave-wave interactions within the wavepacket. The perspective provided by our wavepacket analysis reveals that, ignoring dispersion, this return flow results from an effective mass source-sink dipole acting at the upper boundary of an irrotational fluid.

The total wave-induced flow associated with surface waves is the sum of the divergent-flux induced flow and the return flow: $\vec{U}^{(2)} = U_{\mathrm{DF}}\hat{x} + \vec{U}_{\mathrm{RF}}$, where $\hat{x}$ is the unit-vector in the x-direction.

B. Horizontally periodic internal waves

Plane periodic two-dimensional internal waves in Boussinesq fluid have a dispersion relation $\omega = Nk_x/|\vec{k}|$, in which $\vec{k} = (k_x, k_z)$ is the wavenumber vector and $N = \sqrt{-(g/\rho_0)d\bar{\rho}/dz}$ is the buoyancy frequency, which is a function of the background density gradient $\bar{\rho}$. The polarization relations for these waves expressed in terms of the vertical-displacement amplitude A_0 give the velocities:

$$u = \imath \frac{k_z}{k_x} \omega A_0 e^{\imath(k_x x + k_z z - \omega t)}, \tag{10a}$$

$$w = -\imath \omega A_0 e^{\imath(k_x x + k_z z - \omega t)}. \tag{10b}$$

Using these expressions to compute the Lagrangian horizontal displacement of fluid parcels at order amplitude-squared, as in (3), gives zero. Thus there is no Stokes drift for internal waves.

However, from the energy density, $\mathcal{E} = \rho_0 N^2 {A_0}^2/2$, one can determine the pseudomomentum:

$$\mathcal{P} \equiv \frac{k_x}{\omega}\mathcal{E} = \mathrm{sgn}(k_x)\frac{1}{2}\rho_0 N |\vec{k}| {A_0}^2, \tag{11}$$

in which $\mathrm{sgn}(k_x)$ denotes the sign of the horizontal wavenumber. And so one can infer a corresponding induced flow:

$$u_P \equiv \mathrm{sgn}(k_x)\frac{1}{2} N |\vec{k}| {A_0}^2. \tag{12}$$

From Hamiltonian fluid mechanics[16] or through consideration of the circulation associated with isopycnals displaced by periodic internal waves (cf Sec. 3.4.5 of Sutherland[18]), the wave-induced flow is alternately expressed by $-\langle \xi\zeta\rangle_x$, the negative correlation of the vertical displacement (ξ) and spanwise vorticity (ζ) fields. Using the polarization relations, it is straightforward to show that this expression is equivalent to that given by u_P in (12).

As above, we reconsider this problem by examining the evolution of quasi-monochromatic internal wavepackets[6,7] (cf Sec. 3.4.5 of Sutherland[18]). In this section, we suppose the wavepacket is horizontally periodic but vertically localized with vertical displacement field is given by

$$\xi^{(1)} = A(Z,T)e^{\imath(k_x x + k_z z - \omega t)}, \tag{13}$$

in which $A(Z,T)$ is the (complex) amplitude envelope of the wavepacket that translates at the vertical group velocity c_{gz}, as represented by the choice of the slow scale $Z = \epsilon_z(z - c_{gz}t)$, in which $\epsilon_z \equiv 1/(k_x\sigma_z)$ where σ_z measures the vertical extent of the wavepacket. The effects of dispersion, which come in at higher order in ϵ_z, are expressed through the long time scale $T = \epsilon_z^2 t$.

As in (10b), the corresponding horizontal and vertical velocity fields at leading order in ϵ are

$$u^{(1)} = \imath\frac{k_z}{k_x}\omega A(Z,T)\, e^{\imath(k_x x + k_z z - \omega t)}, \tag{14a}$$

$$w^{(1)} = -\imath\omega A(Z,T)\, e^{\imath(k_x x + k_z z - \omega t)}, \tag{14b}$$

in which it is understood the actual fields are the real parts of the expressions on the right-hand side. Again we consider the flux-form of the horizontal momentum equation (7). Because the wavepacket is horizontally periodic, the x-average of (7) gives the usual expression for momentum transport per unit mass:

$$\frac{\partial}{\partial t}\langle u\rangle_x = -\frac{\partial}{\partial z}\langle uw\rangle_x. \tag{15}$$

It is important to appreciate that u on the left-hand side of (15) does not represent the fluctuation horizontal velocity due to waves. If it were, the average would give zero. Instead $\langle u\rangle_x$ represents the horizontal mean flow that is induced by a wavepacket whose amplitude envelope varies in the vertical. This is not the irreversible mean flow that results from wave breaking. Rather, it is transient: it translates with the vertical group velocity of the wavepacket, the flow accelerating at the wavepacket's leading edge and decelerating at its trailing edge according to (15).

With this in mind, we expect $\langle u\rangle_x$ to depend upon the slow variables Z and T. And so, continuing the informal separation of scales argument, the time derivative on the left-hand side of (15) is replaced by Z and T derivatives according to $\partial_t = -\epsilon_z c_{gz}\partial_Z + \epsilon_z^2\partial_T$, and the second of these is neglected under the assumption that ϵ_z is small. Likewise, $\partial/\partial z$ on the right-hand side of (15) becomes the slow vertical derivative $\epsilon_z\partial_Z$. And so we have to leading order in ϵ_z:

$$\langle u^{(2)}\rangle_x = \frac{1}{c_{gz}}\langle u^{(1)}w^{(1)}\rangle_x. \tag{16}$$

The induced mean flow $\langle u^{(2)}\rangle$ is $O(\alpha^2)$, hence the superscript. Note that (16) is analogous to the well-known result that the mean energy of a wave times its group velocity is just the energy flux. Multiplying both sides of (16) by the background density ρ_0 and by c_{gz} gives the statement that the horizontal momentum times the vertical group velocity equals the vertical flux of horizontal momentum.

Substituting the horizontal and vertical velocities from (14b), we obtain an explicit expression for the divergent-flux induced flow in terms of the amplitude envelope of the vertical displacement field:

$$u_{\mathrm{DF}} \equiv \langle u^{(2)}\rangle_x = \mathrm{sgn}(k_x)\frac{1}{2}N|\vec{k}|\,|A|^2. \tag{17}$$

For vertically as well as horizontally periodic waves, $A(Z,T) = A_0$, in which case u_{DF} reduces to the formula (12) for the wave-induced mean flow derived from the pseudomomentum. Because (17) was derived for horizontally periodic wavepackets, u_{DF} is independent of x and so itself is a

divergence-free flow. Indeed, being derived from the horizontally averaged horizontal momentum equation (15), we see there is no additional induced flow that would result from an order amplitude-squared pressure field. For horizontally periodic internal wavepackets, the divergent-flux induced flow (hence the pseudomomentum per unit mass) is the total wave-induced flow.

III. HORIZONTALLY LOCALIZED INTERNAL WAVEPACKETS

A. The divergent-flux induced flow

Vertically and horizontally localized wavepackets translate in the x-z plane at the group velocity $\vec{c}_g = (c_{gx}, c_{gz})$. As such, in addition to the slow variable $Z = \epsilon_z(z - c_{gz}t)$ used above, we introduce the slow scale in a frame translating at the horizontal group velocity $X = \epsilon_x(x - c_{gx}t)$, in which $\epsilon_x \equiv 1/(k_x\sigma_x)$ and σ_x measures the horizontal extent of the wavepacket. For convenience, we suppose $\sigma \equiv \sigma_x \sim \sigma_z$ so that $\epsilon \equiv \epsilon_x \sim \epsilon_z$. The slow variables are thus defined to be

$$X = \epsilon(x - c_{gx}t), \tag{18a}$$

$$Z = \epsilon(z - c_{gz}t), \tag{18b}$$

$$T = \epsilon^2 t. \tag{18c}$$

Similar to (13), the leading-order vertical displacement field is

$$\xi_0^{(1)} = A(X, Z, T)e^{i(k_x x + k_z z - \omega t)}, \tag{19}$$

in which the subscript and superscript emphasize that the term is $O(\epsilon^0\alpha^1)$. Corresponding expressions for the horizontal and vertical velocity are found as in (14b), respectively, but with the arguments to A additionally involving the slow variable X.

The flux-form of the horizontal momentum equation is again given by (7). But now we cannot meaningfully average in the horizontal. Neglecting pressure for now, we focus on the flow resulting from the vertical divergence of the horizontal momentum flux u_{DF}:

$$\partial_t u_{\mathrm{DF}} = -\partial_x \overline{u_0^{(1)} u_0^{(1)}} - \partial_z \overline{u_0^{(1)} w_0^{(1)}}. \tag{20}$$

As in (8), the over-line denotes the operation of effectively averaging with respect to the fast scales keeping only the slow variations.

Following the same procedure, we write the vertical momentum equation in flux-form and consider the slowly varying, order amplitude-squared terms crucially neglecting the mean pressure gradient and buoyancy forcing that arise at the same order. The resulting equation for the vertical component of the divergent-flux induced flow is thus given by

$$\partial_t w_{\mathrm{DF}} = -\partial_x \langle u_0^{(1)} w_0^{(1)} \rangle - \partial_z \langle w_0^{(1)} w_0^{(1)} \rangle. \tag{21}$$

We now recast these equations in terms of the slow variables, keeping terms of order ϵ alone. In particular, at $O(\epsilon)$, the partial time-derivative on the left-hand sides of (20) and (21) becomes $\partial_t \sim -\epsilon c_{gx}\partial_X - \epsilon c_{gz}\partial_Z$. Thus, we arrive at the pair of equations

$$\vec{c}_g u_{\mathrm{DF}} = \overline{u_0^{(1)} \vec{u}_0^{(1)}}, \tag{22a}$$

$$\vec{c}_g w_{\mathrm{DF}} = \overline{w_0^{(1)} \vec{u}_0^{(1)}}. \tag{22b}$$

Finally, using the polarization relations of the form (14b), we derive an explicit expression for the divergent-flux induced flow of horizontally and vertically localized internal gravity wavepackets:

$$(u_{\mathrm{DF}}, w_{\mathrm{DF}}) = \mathrm{sgn}(k_x)\frac{1}{2c_{gx}} N|\vec{k}|\,|A|^2 \vec{c}_g = \mathrm{sgn}(k_x)\frac{1}{2} N|\vec{k}|\,|A|^2 \left(1, -\frac{k_z}{k_x}\right). \tag{23}$$

The horizontal component is the same as that found for horizontally periodic wavepackets in (17). But it is now evident that the divergent-flux induced flow has a vertical component as well.

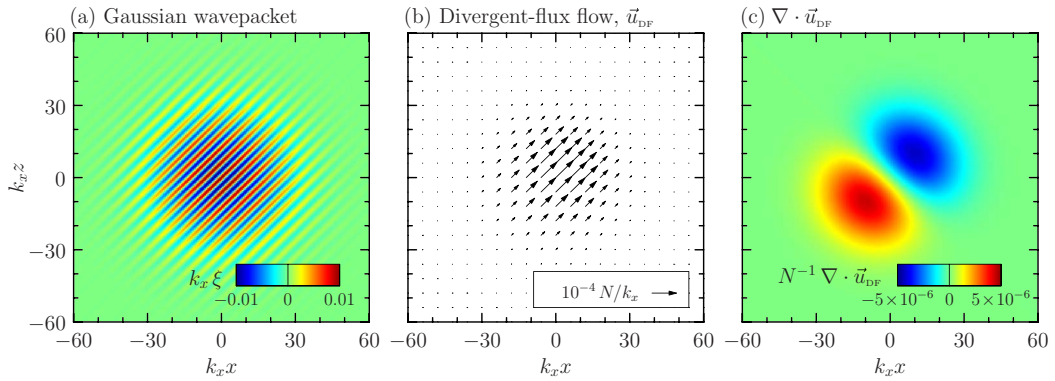

FIG. 1. (a) Vertical displacement field associated with a localized internal wavepacket defined to propagate upward and to the right, (b) its corresponding divergent-flux induced flow given by (23), and (c) the negative divergence of this induced flow field. The wavepacket is defined with $\vec{k} = k_x(1,1)$, envelope width $\sigma = \sigma_x = \sigma_z = 20k_x^{-1}$ and amplitude $A_0 = 0.01k_x^{-1}$. The legend in (b) indicates the magnitude of the displayed arrow.

By way of illustration, Figures 1(a) and 1(b) show the vertical displacement field and divergent-flux induced flow associated with a Gaussian wavepacket centred at the origin whose vertical displacement field is given by

$$\xi = A_0 \exp\left[-\frac{1}{2}\left(\frac{x^2}{{\sigma_x}^2} + \frac{z^2}{{\sigma_z}^2}\right)\right] \cos(k_x x + k_z z), \tag{24}$$

with $k_z = -k_x$, $\sigma_x = \sigma_z = 20{k_x}^{-1}$, and $A_0 = 0.01{k_x}^{-1}$. The divergent-flux induced flow in Figure 1(b) is negligible except within the wavepacket itself and the direction of the flow is everywhere parallel to the group velocity vector.

Unlike the case of horizontally periodic waves, (23) cannot represent the total wave-induced flow. Computing the negative divergence of (23), shown in Figure 1(c), we see that there is a net transport of mass away from the trailing edge of the packet and a net deposition of mass at the leading edge. The flow is not divergence free. So, as in the case of horizontally localized surface gravity wavepackets, there must be a response flow that results in a divergence-free total wave-induced flow.

B. Total wave-induced flow and leading-order response flow

Here we derive an expression that predicts the leading-order, divergence-free, wave-induced flow that is the sum of the divergent-flux induced flow (23) and the response flow. After finding the total flow, it is straightforward to find the response flow.

We first manipulate the fully nonlinear equations describing motion in a uniformly stratified, Boussinesq fluid. Neglecting diffusion, the internal energy equation is $D\rho_T/Dt = 0$, in which $\rho_T = \bar{\rho}(z) + \rho(x, z, t)$ is the background $\bar{\rho}(z)$ plus perturbation density $\rho(x, z, t)$ and D/Dt is the material derivative. This is recast in terms of the vertical displacement field using

$$\xi = -\rho/\bar{\rho}', \tag{25}$$

in which the prime denotes the z-derivative. Thus the internal energy equation is written

$$\frac{D\xi}{Dt} = w. \tag{26}$$

Taking the curl of the momentum equations conveniently eliminates pressure and gives the equation for the evolution of spanwise vorticity:

$$\frac{D\zeta}{Dt} = N^2 \frac{\partial \xi}{\partial x}. \tag{27}$$

Being an incompressible fluid, the velocity fields can be written in terms of gradients of the streamfunction, ψ:

$$u = -\partial\psi/\partial z \tag{28a}$$

and

$$w = \partial\psi/\partial x, \tag{28b}$$

and the vorticity is related to the streamfunction through

$$\zeta = -\nabla^2\psi. \tag{29}$$

Finally, we combine (26) and (27) to give a differential equation written in terms of a linear differential operator L acting on ψ on the left-hand side and the divergence of a nonlinear vector $\vec{F}$ on the right-hand side

$$\underbrace{\left[\partial_{tt}(\partial_{xx}+\partial_{zz})+N^2\partial_{xx}\right]}_{\equiv L}\psi = \nabla\cdot\underbrace{\left[\partial_t\left(\zeta\,\vec{u}\right)+N^2\partial_x\left(\xi\,\vec{u}\right)\right]}_{\equiv\vec{F}}. \tag{30}$$

Equations (26) and (30), together with (29) and (28), comprise the two coupled fully nonlinear governing equations in ξ and ψ.

As in Sec. III A, we consider a horizontally and vertically localized wavepacket whose vertical displacement field $\xi_0^{(1)}$ is given by (19), in which the slow variables are defined by (18). The polarization relations of plane waves give corresponding formulae at first order in amplitude for the velocity $\vec{u}_0^{(1)}$ and the vorticity $\zeta_0^{(1)}$. Substituting these relations in the right-hand side of (30), gives the second-order amplitude equation:

$$L\psi^{(2)} = \nabla\cdot\left[\partial_t\left(\zeta^{(1)}\vec{u}^{(1)}\right)+N^2\partial_x\left(\xi^{(1)}\vec{u}^{(1)}\right)\right], \tag{31}$$

where the linear operator L is defined in (30) and, for now, we have included terms at all orders in ϵ arising from the various slow derivatives. If we substitute plane-wave solutions, for which $A(X, Z, T) = A_0$ is constant, into the right-hand side of (31), we find the operator is identically zero. This demonstrates the well-known result that plane periodic internal gravity waves satisfy the nonlinear equations exactly. The total wave-induced flow, derived from the $O(\alpha^2)$ streamfunction $\psi^{(2)}$, is a consequence of the internal wavepacket having finite spatial extent as expressed by the small but non-zero value of ϵ.

However, if we use the $O(\alpha^1\epsilon^0)$ wavepacket formulae for $\xi_0^{(1)}$, $\zeta_0^{(1)}$, and $\vec{u}_0^{(1)}$, as in (19), to compute the slowly varying products $\overline{\zeta_0^{(1)}\vec{u}_0^{(1)}}$ and $\overline{\xi_0^{(1)}\vec{u}_0^{(1)}}$ in (31), again we get zero. This is because the vertical displacement and vorticity fields associated with plane waves are 90° out of phase with the components of the velocity field. As shown in Sec. III D and the Appendix, the leading non-zero terms resulting from the products of vorticity and vertical displacement with velocity are $O(\alpha^2\epsilon)$. Therefore, the scales of each term in (31) are given as follows:

$$\Big[\underbrace{\partial_{tt}\left(\partial_{xx}+\partial_{zz}\right)}_{O(\alpha^0\epsilon^4)}+\underbrace{N^2\partial_{xx}}_{O(\alpha^0\epsilon^2)}\Big]\underbrace{\psi^{(2)}(X,Z)}_{O(\alpha^2\epsilon^0)} = \underbrace{\nabla\cdot\left[\partial_t\left(\zeta^{(1)}\,\vec{u}^{(1)}\right)+N^2\partial_x\left(\xi^{(1)}\,\vec{u}^{(1)}\right)\right]}_{O(\alpha^2\epsilon^3)}, \tag{32}$$

where we have assumed the divergence on the right-hand side induces a response expressed in terms of the streamfunction $\psi^{(2)}$, which is a function of the slow scales X and Z. Extracting the leading-order term, gives the differential equation $\epsilon^2\partial_{XX}\psi^{(2)}(X, Z) = 0$, which has the general solution:

$$\psi^{(2)} = f(Z)X - g(Z),$$

where $f(Z)$ and $g(Z)$ are arbitrary functions of the slow scale Z. Using (28), we find that the general velocity field for the leading-order total wave-induced flow in a frame of reference moving with the wavepacket is $(u^{(2)}, w^{(2)}) = \left(-f'(Z)X + g'(Z),\, f(Z)\right)$. Requiring bounded horizontal flows as $X \to \pm\infty$, we must have $f'(Z) = 0$. And so $f(Z)$ is constant. But the additional requirement that the

wave-induced vertical velocity must be zero as $Z \to \pm\infty$ means $f(Z) = 0$. Therefore, at this order of approximation the total wave-induced flow is

$$u^{(2)} = G(Z), \tag{33a}$$

$$w^{(2)} = 0, \tag{33b}$$

in which $G(Z) \equiv g'(Z)$ is some function of Z. Thus we have shown that at $O(\alpha^2\epsilon^1)$ the total wave-induced flow has no vertical motion but extends horizontally far from the wavepacket.

These equations for the total wave-induced flow, together with Eq. (23) for the divergent-flux induced flow of internal waves, gives formulae for the response flow ($u_{\rm RF}$, $w_{\rm RF}$). To satisfy (33b), we must have

$$w_{\rm RF} = -w_{\rm DF} = \frac{1}{2}\frac{N^2 k_z}{\omega}\,|A|^2.$$

Because the total horizontal wave-induced flow $u^{(2)} = G(Z)$ is independent of x, momentum conservation dictates that the response flow at this order must act to spread the local divergent-flux induced flow $u_{\rm DF}$ horizontally uniformly in x. Explicitly, the horizontal component of the response flow is

$$u_{\rm RF} = -u_{\rm DF} + \frac{1}{L_x}\int u_{\rm DF}\,dx,$$

in which the integral is performed over the horizontal extent of the domain L_x. Combining these results, the total wave-induced flow at $O(\alpha^2\epsilon)$ is

$$\vec{u}^{(2)} = \left(\frac{1}{L_x} I_{u,\rm DF},\, 0\right), \tag{34}$$

in which

$$I_{u,\rm DF} = \int u_{\rm DF}\,dx \tag{35}$$

is the horizontally integrated horizontal component of the divergent-flux induced flow. In particular, for a Gaussian wavepacket centred at the origin with vertical displacement given by (24), Eqs. (23) and (35) give

$$I_{u,\rm DF} = \mathrm{sgn}(k_x)\frac{1}{2}\sqrt{\pi}\,\sigma_x\; N|\vec{k}|A_0^2\, e^{-z^2/\sigma_z{}^2}. \tag{36}$$

C. Horizontal long wave response: Scaling considerations

At first glance, (34) suggests the counter-intuitive prediction that the wave-induced flow decreases to zero as the horizontal extent of the domain in which the wavepacket propagates extends to infinity. Yet, it must be kept in mind that the prediction (33) arises as a result of truncating the perturbation expansion on the right-hand side of (32) at $O(\alpha^2\epsilon^2)$. As we will show in Sec. III D, by considering terms at $O(\alpha^2\epsilon^3)$ on the right-hand side of (32), the wave-induced flow at higher order in ϵ is in fact a horizontally long internal wave that translates vertically with the wavepacket.

This insight does not negate the usefulness of results in Sec. III B. In the wavepacket''s immediate surroundings, the wave-induced flow does appear to be horizontally uniform. Only in the far field to either side of the wavepacket does the horizontal flow gradually decrease to zero. Nonetheless, the horizontal extent of the induced flow is finite. And so it is not useful to compute the average of a localized horizontal flow over the domain as in (34). It is useful, however, to characterize the magnitude of the induced horizontal flow in terms of the integral given by (35). Here we use this diagnostic and physical reasoning to make order-of-magnitude estimates for the structure of the long wave induced by the wavepacket. The estimates will be compared with the long wave properties derived more rigorously in Sec. III D.

We imagine the wavepacket as a translating body force in a stratified ambient that excites a long, hence hydrostatic, internal wave. This part of the induced flow we describe as the "response

wave." Its spatiotemporal structure (denoted by "r" subscripts) is described by the following three relationships:

$$\omega_r = N\frac{k_{xr}}{|k_{zr}|}, \tag{37a}$$

$$\frac{\omega_r}{k_{zr}} = c_{gz}, \tag{37b}$$

$$|k_{zr}| \simeq \frac{2\pi}{4\sigma_z}. \tag{37c}$$

The first identity is the dispersion relation for long waves ($|k_{xr}| \ll |k_{zr}|$). The second identity equates the vertical phase speed of the response wave to the vertical group velocity of the localized wavepacket c_{gz}, which is the source of the response waves. Finally, assuming the localized wavepacket travels rightward, the horizontal velocity field associated with the response wave near the localized wavepacket must positive over the total vertical extent $\sim 2\sigma_z$ of the localized wavepacket. This gives rise to the third expression for the approximate vertical wavenumber of the response wave.

Combining the expression in (37) gives the horizontal wavenumber of the response wave and the lateral extent of the disturbance L_i, estimated to be half a horizontal wavelength of the response wave:

$$|k_{xr}| = \frac{|c_{gz}|}{N}k_{zr}^2 \simeq \left(\frac{\pi^2}{4}\frac{k_x^2|k_z|}{|\vec{k}|^3}{\epsilon_z}^2\right)k_x, \tag{38a}$$

$$L_i = \pi/|k_{xr}| \simeq \left(\frac{4}{\pi}\frac{|\vec{k}|^3}{k_x^2|k_z|}\,\epsilon_x{\epsilon_z}^{-2}\right)\sigma_x. \tag{38b}$$

The scaling for $|k_{xr}|$ emphasizes that the response wave is long compared to the horizontal wavenumber of the waves k_x, and the scaling for L_i emphasizes that the horizontal extent of the long wave is indeed much wider than the wavepacket extent σ_x, under the assumption that $\epsilon_x \sim \epsilon_z$. The scaling relationship for L_i is alternately found by considering the distance travelled by a long wave at its horizontal group velocity $|c_{gxr}| \simeq N|k_{xr}|/{k_{zr}}^2$ over the time, σ_z/c_{gz}, in which the wavepacket travels vertically at its group velocity over its vertical extent. Likewise, by examining characteristic velocity and time scales, Bretherton[1] proposed the scaling $L_i \sim \epsilon^{-1}N{\sigma_z}^2/c_{gz}$, in which $\epsilon = \epsilon_x \sim \epsilon_z$. By matching the dispersion characteristics of the wavepacket and the response wave, (38) is more explicit in the dependence of L_i upon the vertical and horizontal extents of the wavepacket.

The response wave should emanate from the localized wavepacket qualitatively like a bow wave. The corresponding magnitude of the slope of lines of constant phase of the response wave is

$$\left|\frac{k_{xr}}{k_{zr}}\right| = \frac{\pi}{2}\cos^2\theta\,\sin|\theta|\,\epsilon_z, \tag{39}$$

which, being small, is consistent with this being a long wave.

The amplitude of the response wave is estimated by the requirement that the horizontal integral of the horizontal flow over a crest of the long wave should equal $I_{u,\,\mathrm{DF}}$, given by (35). Thus the amplitude of the horizontal velocity associated with the long wave is

$$A_{0ur} \simeq \frac{1}{2}k_{xr}I_{u,\mathrm{DF}}. \tag{40}$$

In particular, for the Gaussian wavepacket given by (24), we estimate

$$A_{0ur} \simeq \frac{\pi^2}{16}(\sqrt{\pi}\sigma_x)\frac{Nk_x^3|k_z|}{|\vec{k}|^2}\,|A_0|^2{\epsilon_z}^2 = \frac{\pi^{5/2}}{16}\frac{N|k_z|}{|\vec{k}|^2}\,\alpha^2{\epsilon_x}^{-1}{\epsilon_z}^2, \tag{41}$$

in which we have used (36). Because the divergent-flux induced flow has spread laterally over a distance of order L_i, the total wave-induced flow within the wavepacket, estimated by A_{0ur}, is smaller than u_{DF} by a factor ${\epsilon_x}^{-1}{\epsilon_z}^2$.

D. Estimation of the horizontal long wave response

In Sec. III B we derived the fully nonlinear equation (30) expressed in terms of a linear response $L\psi$ to nonlinear forcing $\nabla \cdot \vec{F}$. There we showed that substitution of the leading order fields associated with the wavepacket into the quadratic terms of $\vec{F}$ gives zero. One must express the fields associated with the wavepacket to next order in ϵ in order to produce a non-trivial nonlinear forcing term. The details of this calculation are provided in the Appendix. Therein we derive expressions for $\vec{u}$, ξ, and ζ at $O(\alpha^1\epsilon^1)$ and from these we find $\nabla \cdot \vec{F}$ at $O(\alpha^2\epsilon^3)$.

With the insight provided in Sec. III C, we expect the nonlinear forcing given by (A4) to excite a disturbance that is long compared to the horizontal extent of the forcing region. Following Bretherton,[1] we therefore approximate the x-dependent forcing by a Dirac delta function. Explicitly, we write the nonlinear forcing term as

$$(\nabla \cdot \vec{F})_3^{(2)} \simeq \mathcal{N}(\tilde{z})\delta(k_x\tilde{x}), \tag{42}$$

in which

$$\mathcal{N}(\tilde{z}) = k_x \int_{-\infty}^{\infty} (\nabla \cdot \vec{F})_3^{(2)}\, d\tilde{x}. \tag{43}$$

For later convenience, we have written the result in terms of the fast variables in a reference frame translating at the group velocity of the wavepacket $\tilde{x} = X/\epsilon = x - c_{gx}t$ and $\tilde{z} = Z/\epsilon = z - c_{gz}t$. In particular, if the amplitude envelope of the vertical displacement field is a Gaussian in the horizontal so that $A(\tilde{x}, \tilde{z}) = A_0 \exp[-\tilde{x}^2/(2\sigma_x^2)]\, \mathcal{A}(\tilde{z})$ with $||\mathcal{A}|| = 1$, then (43) together with (A4) gives

$$\mathcal{N}(\tilde{z}) = -\frac{1}{2}(\sqrt{\pi}\,\sigma_x)\, N^3 \frac{k_x^3 k_z^2}{|\vec{k}|^5} A_0^2 \partial_{\tilde{z}\tilde{z}\tilde{z}} |\mathcal{A}|^2. \tag{44}$$

In deriving this result we note that the integral in $\tilde{x}$, hence in X, eliminates all terms in (A4) that involve at least one X derivative. The term that remains results from the vertical divergence of $\partial_t(\overline{\zeta w})$. Transforming from Z- to $\tilde{z}$-derivatives results in the implicit appearance of $\epsilon_z^3 = (k_x\sigma_z)^{-3}$.

To find the induced long wave response at $O(\alpha^2)$ to the nonlinear forcing of a horizontally Gaussian wavepacket, we solve for the streamfunction $\psi^{(2)}$ by substituting (42) and (44) on the right-hand side of (30). On the left-hand side we solve in the vertically translating frame and make use of the long wave approximation so that $\partial_{tt} \sim c_{gz}^2\partial_{\tilde{z}\tilde{z}}$ and $\partial_{xx} + \partial_{zz} \sim \partial_{\tilde{z}\tilde{z}}$. Explicitly, we have

$$\left(c_{gz}^2\partial_{\tilde{z}\tilde{z}\tilde{z}\tilde{z}} - N^2\partial_{\tilde{x}\tilde{x}}\right)\psi^{(2)} = \mathcal{N}(\tilde{z})\delta(k_x\tilde{x}). \tag{45}$$

The solution is found by taking the double Fourier transform in $\tilde{x}$ and $\tilde{z}$ of the resulting differential equation. We begin by taking the Fourier transform of the right-hand side (42) with $\mathcal{N}(\tilde{z})$ given by (44):

$$\int_{-\infty}^{\infty}\int_{-\infty}^{\infty} (\nabla \cdot \vec{F})_3^{(2)} e^{-\imath(\kappa\tilde{x}+\mu\tilde{z})} d\tilde{x}d\tilde{z} = \frac{\imath\pi}{2} N^3 \frac{k_x^2 k_z^2}{|\vec{k}|^5} A_0^2\sigma_x\sigma_z\, \mu^3 \widehat{|\mathcal{A}|^2}, \tag{46}$$

in which $\widehat{|\mathcal{A}|^2}(\mu)$ is the Fourier transform of $|\mathcal{A}|^2(\tilde{z})$. In particular, if the wavepacket is a Gaussian in the vertical as well as horizontal such that $\mathcal{A} = \exp(-z^2/2\sigma_z^2)$, we have the Fourier transform pair

$$|\mathcal{A}|^2 = \exp(-\tilde{z}^2/\sigma_z^2), \quad \widehat{|\mathcal{A}|^2} = \exp(-(\mu\sigma_z)^2/4). \tag{47}$$

The solution to (45) in Fourier space is given generally by

$$\hat{\psi}^{(2)}(\kappa, \mu) = \frac{\imath\pi}{2} N^3 \frac{k_x^2 k_z^2}{|\vec{k}|^5} A_0^2\sigma_x\sigma_z \frac{\mu^3 \widehat{|\mathcal{A}|^2}}{c_{gz}^2\mu^4 - N^2\kappa^2}. \tag{48}$$

While inverting the double Fourier transform to obtain the solution for $\psi^{(2)}$ in real space, the integral with respect to κ can be evaluated explicitly. In doing so, it is necessary to select the branch cut corresponding to outgoing waves.[1] Thus we find

$$\psi^{(2)}(\tilde{x}, \tilde{z}) = -\frac{1}{8} N \frac{k_x k_z}{|\vec{k}|^2} A_0^2\sigma_x\sigma_z \int_0^{\infty} \widehat{|\mathcal{A}|^2}\mu \cos\left(\mu z + \mu^2 \frac{c_{gz}|x|}{N}\right) d\mu, \tag{49}$$

which corresponds to the solution given by (3.15-3.16) in Bretherton.[1] Therefore, the horizontal flow associated with the induced long wave is

$$u^{(2)}(\tilde{x},\tilde{z}) = -\frac{1}{8}N\frac{k_x k_z}{|\vec{k}|^2}A_0^2\sigma_x\sigma_z\int_0^\infty \widehat{|\mathcal{A}|^2}\mu^2\sin\left(\mu z + \mu^2\frac{c_{gz}|x|}{N}\right)d\mu. \tag{50}$$

In particular, for a bivariate Gaussian wavepacket, according to (47) we have

$$\psi^{(2)}(\tilde{x},\tilde{z}) = -\frac{1}{8}N\frac{k_x k_z}{|\vec{k}|^2}A_0^2\frac{\sigma_x}{\sigma_z}\int_0^\infty e^{-\tilde{\mu}^2/4}\tilde{\mu}\cos\left(\tilde{\mu}\frac{\tilde{z}}{\sigma_z} + \tilde{\mu}^2\frac{c_{gz}|x|}{N\sigma_z^2}\right)d\tilde{\mu} \tag{51}$$

and

$$u^{(2)}(\tilde{x},\tilde{z}) = -\frac{1}{8}N\frac{k_x k_z}{|\vec{k}|^2}A_0^2\frac{\sigma_x}{\sigma_z^2}\int_0^\infty e^{-\tilde{\mu}^2/4}\tilde{\mu}^2\sin\left(\mu\frac{z}{\sigma_z} + \tilde{\mu}^2\frac{c_{gz}|x|}{N\sigma_z^2}\right)d\tilde{\mu}. \tag{52}$$

Figure 2 plots the predicted streamfunction and horizontal velocity associated with the long wave induced by an upward-propagating Gaussian wavepacket given by (24). Clearly, the induced wave is significantly longer than the horizontal extent of the wavepacket, which is $\sigma_x = 20k_x^{-1}$. From (38b), the predicted horizontal extent of the wavepacket is $L_i \simeq 1440k_x^{-1}$, which is a reasonable estimate of the lateral extent of the induced long waves to either side of the wavepacket at $z = 0$. Below the wavepacket the induced long waves extend much further laterally, spreading in a manner qualitatively similar to that of a bow wake.

Crucially, these lee waves have zero net horizontal flow associated with them. Even though the induced long wave has alternating positive and negative horizontal velocity field, as anticipated from the results in Sec. III B these cancel upon integration except at the level of the wavepacket itself. This can be shown by horizontally integrating (50):

$$\int_{-\infty}^{\infty}u^{(2)}\,dx = N|\vec{k}|(\sqrt{\pi}\sigma_x)\int_0^\infty \widehat{|\mathcal{A}|^2}\cos(\hat{m}\tilde{z})\,d\hat{m} = \frac{1}{2}N|\vec{k}|(\sqrt{\pi}\sigma_x)\,|\mathcal{A}|^2. \tag{53}$$

This is equal to the horizontal integral of the horizontally integrated divergent-flux flow given generally by (23) and (35), and given explicitly by (36) for a wavepacket that is Gaussian in the vertical and horizontal. The result is plotted as the thick solid line in Figure 2(c).

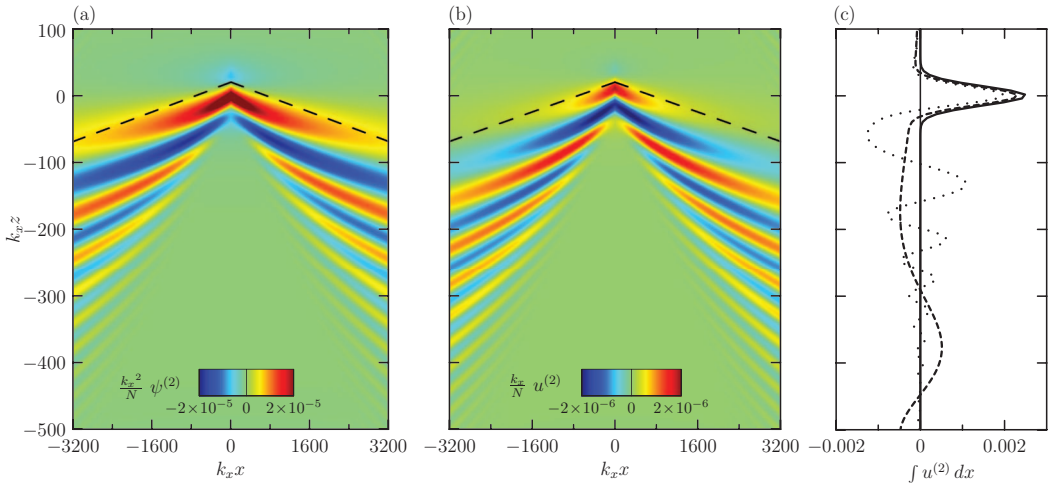

FIG. 2. Predicted (a) streamfunction and (b) horizontal velocity field of the long wave induced by a Gaussian wavepacket centred at the origin with $k_z = -k_x$, $k_x\sigma_x = k_x\sigma_z = 20$, and $k_x A_0 = 0.01$. The diagonal dashed lines in (a) and (b) indicate the predicted slope of phase lines of the long wave according to (39). Panel (c) shows the horizontal integral of the horizontal velocity predicted by theory (solid line) and computed numerically in a finite sized domain with $-500 \le k_x z \le 100$ and $-3217 \le k_x x \le 3217$ (dotted line) and with $-5500 \le k_x z \le 500$ and $-25736 \le k_x x \le 25736$ (dashed line).

Although the horizontally integrated flow is strictly positive, the local horizontal flow about the wavepacket itself changes sign in the vertical. In particular, from (52) a wavepacket with bivariate Gaussian amplitude envelope has an induced horizontal velocity profile along its horizontal center given by

$$u^{(2)}(\tilde{x}=0,\tilde{z}) = \frac{1}{2}N\frac{k_x k_z}{|\vec{k}|^2}A_0^2\frac{\sigma_x}{\sigma_z^2}\Big[-\frac{\tilde{z}}{\sigma_z} + \Big(2\big(\frac{\tilde{z}}{\sigma_z}\big)^2 - 1\Big)\,D(\tilde{z}/\sigma_z)\Big], \tag{54}$$

in which $D(x) = e^{-x^2}\int_0^x e^{t^2}\,dt = (1/2)\int_0^\infty e^{-t^2/4}\sin(xt)\,dt$ is Dawson's integral.[21] Because $D(x)$ is an odd function, it is evident that $u^{(2)}$ is zero at the vertical center of the wavepacket, begin positive above and negative below if the wavepacket propagates upward and to the right. This result has potentially important consequences for the modulational stability of moderately large amplitude internal wavepackets. The stability of horizontally periodic Boussinesq internal waves was assessed through the derivation of a nonlinear Schrödinger equation in which the nonlinear term was strictly positive as a consequence of the wave-induced mean flow being positive.[6] Though beyond the scope of this paper, future work will consider the weakly nonlinear influence upon a wavepacket of an induced horizontal flow that changes sign over its vertical extent.

Finally, we comment upon the implementation of these results in numerical simulations. For this purpose, the Fourier transforms in (51) and (52) must be estimated by computing Fourier series in a finite sized domain. Because the lee wave, shown, for example, in Figure 2(b), has significant amplitude far from the wavepacket, this means that the inverse transform must be computed on a very wide and deep domain in order to reproduce properly the horizontally integrated horizontal flow. To illustrate this, in Figure 2(c) we also plot the horizontally integrated, horizontal flow found by inverse transforming (52) on two different sized domains. In a domain with the horizontal and vertical extent of the fields plotted in Figures 2(a) and 2(b), the horizontally integrated horizontal velocity is moderately smaller than that predicted by (36) about the level of the wavepacket and at greater depths it alternates between positive and negative flows whose magnitude decreases with vertical distance away from the wavepacket. These result because the lee wave is significant at the sides of the domain. If the domain is much wider (over 200 times the wavepacket width), the computed horizontally integrated flow is closer to the prediction (36) and there is better cancellation of the positive and negative flows with depth.

Although accurate numerical calculation of the integrated horizontal velocity requires a large domain, the streamfunction, horizontal velocity, and other fields associated with the long wave change negligibly about the location of the wavepacket if the domain is sufficiently wide (i.e., about $4L_i$) and sufficiently deep so that the trailing waves have negligible amplitude at the bottom of the domain.

All of this is to say that numerical simulations of a wavepacket that include the predicted lee wave as an initial condition would have to be performed on (perhaps impractically) large domains in order to give an accurate representation of the momentum transport expressed through the horizontally integrated horizontal flow. This insight guides the design of the numerical simulations used to test the predictions of theory.

IV. NUMERICAL SIMULATIONS

A. Numerical model and initial conditions

The evolution of internal wavepackets in a uniformly stratified fluid is simulated using a code that solves the fully nonlinear, Boussinesq Navier Stokes equations in two dimensions.[22] Instead of directly solving the momentum equations, the code evolves the spanwise vorticity field $\zeta \equiv (\nabla \times \vec{u})\cdot\hat{y}$, whose evolution equation is found from taking the curl of the momentum equations. As discussed in Sec. III B, instead of considering density perturbations, we evolve the vertical displacement field $\xi \equiv -(\bar{\rho}')^{-1}\rho$ through manipulation of the internal energy equation (26).

Explicitly, ξ and ζ are advanced in time according to the (non-dimensional) equations obtained from (26) and (27) with added viscous damping and thermal diffusion terms:

$$\begin{aligned} \frac{\partial \xi}{\partial t} &= -u\frac{\partial \xi}{\partial x} - w\frac{\partial \xi}{\partial z} + w + \frac{1}{\mathrm{RePr}}\mathcal{D}\xi, \\ \frac{\partial \zeta}{\partial t} &= -u\frac{\partial \zeta}{\partial x} - w\frac{\partial \zeta}{\partial z} + \frac{g}{\rho_0}\frac{\partial \rho}{\partial x} + \frac{1}{\mathrm{Re}}\mathcal{D}\zeta, \end{aligned} \tag{55}$$

in which $\mathcal{D}$ represents a diffusivity operator and we set the Prandtl number to be $\mathrm{Pr} = 1$ and the Reynolds number $\mathrm{Re} \equiv (N/k_x{}^2)/\nu = 10^6$. The effects of diffusivity are included to ensure numerical stability but their influence is set to be negligible as far as the evolution of the wavepacket and induced mean flow is concerned. To minimize the influence of diffusivity upon the wavepacket and wave-induced flow, in the simulations reported upon here, Laplacian diffusivity acts only on disturbances with horizontal wavenumbers much larger than the wavenumber of the localized wavepacket k_x. The equations are solved in a horizontally periodic domain with free-slip upper and lower boundaries. The fields themselves are discretized by Fourier modes in the horizontal and by discrete evenly spaced grid points in the vertical. In this horizontal Fourier space, in which $\partial_x \to \imath k$, the diffusivity operator is expressed by

$$\mathcal{D} = \begin{cases} 0 & k \le k_\star \\ -k^2 + \partial_{zz} & k > k_\star. \end{cases} \tag{56}$$

In the simulations reported upon here we set the cut-off wavenumber to be $k_\star = 2k_x$.

Given ζ, the stream function is found by inverting Poisson's equation $\zeta = -\nabla^2\psi$, which is equivalent to inverting a tri-diagonal matrix in horizontal Fourier space. From ψ, the velocity components are found using (28).

The simulation is initialized by a Gaussian wavepacket whose vertical displacement field in general is given in real-space by

$$\xi(x, z, t = 0) = A(x, z, 0)\ \cos(k_x x + k_z z). \tag{57}$$

In simulations of vertically localized and horizontally periodic wavepackets centred initially at the origin, the amplitude envelope is $A(x, z, 0) = A_0 \exp\left[z^2/(2\sigma_z{}^2)\right]$ and the width of the domain is set to be $\lambda_x = 2\pi/k_x$. In simulations of horizontally and vertically localized wavepackets the amplitude envelope is given as in (24) by $A(x, z, 0) = A_0 \exp\left[x^2/(2\sigma_x{}^2) + z^2/(2\sigma_z{}^2)\right]$ and the width of the domain is set to be very much larger than σ_x. In either case, assuming small amplitude quasi-monochromatic wavepackets, linear theory is used to initialize the corresponding vorticity field through

$$\zeta(x, z, t = 0) = A_\zeta\ \cos(k_x x + k_z z), \tag{58}$$

in which $A_\zeta \equiv N(k_x{}^2 + k_z{}^2)^{1/2}A$.

Here we report upon simulations of the wavepacket examined in Sec. III. Explicitly, using $k_x{}^{-1}$ and N^{-1} to define the characteristic length and time scales, we fix $k_z = -k_x$ and set $A_0 = 0.01k_x{}^{-1}$. According to the dispersion relation, the wave has constant-phase lines oriented at 45° to the vertical and the wavepacket propagates upward to the right at group velocity $(c_{gx}, c_{gz}) = N/(2\sqrt{2}k_x)\,(1, 1)$. The vertical extent of the wavepacket is $\sigma_z = \sigma \equiv 20k_x{}^{-1}$ ($\epsilon_z = 0.05$) and in horizontally localized wavepacket simulations we also set $\sigma_x = \sigma$ ($\epsilon_x = 0.05$).

According to (38), the horizontal extend of the induced long wave is expected to be on the order of $L_i = 3200\sqrt{2}/\pi\ k_x{}^{-1} \simeq 1440k_x{}^{-1}$ on either side of the wavepacket. With this in mind, in simulations of horizontally localized wavepackets the horizontal extent of the domain is set to be $1024\lambda_x = 6434k_x{}^{-1}$. We will show that this is sufficiently wide that the periodic boundary conditions do not affect the wavepacket or the induced mean flow about the level of the wavepacket as it translates upward.

For straightforward comparison of the numerical results with theory, the wavepacket is situated initially with its centre at the origin. Thus, after time $Nt = 200$, the wavepacket is expected to be centred about $(x, z) \simeq (70.7, 70.7)k_x^{-1}$ after propagating diagonally a distance of approximately 5σ. In this location, after the transient start-up time resulting from choosing the initial ambient to be stationary, we may reasonably compare the measured flow induced by the wavepacket with the predictions of steady state theory. This is demonstrated explicitly below in the examination of the

horizontally periodic wavepacket. The upper and lower boundaries of the domain are situated at $z = 200k_x^{-1}$ and $z = -100k_x^{-1}$, sufficiently far that these do not influence the wavepacket evolution over the duration of a simulation.

For horizontally periodic, vertically localized wavepackets, Sutherland[6] showed that one should also superimpose on the perturbation fields the horizontal component of the wave-induced flow, given by (23) for rightward-propagating waves: $u_{\rm DF}(z, t = 0) = -\langle \xi \zeta \rangle_{t=0} = (1/2)N|\vec{k}||A_0(z)|^2$, in which $A_0(z) = A(z, t = 0)$ is the initial amplitude envelope of the vertical displacement field. This is not a steady background flow but the transient induced mean horizontal flow at $t = 0$ that at later times translates vertically at the vertical group velocity with the wavepacket. If a simulation is initialized with zero mean horizontal flow then, by momentum conservation, the vertically integrated mean horizontal momentum must be zero for all time. So the zero mean flow initial condition is actually specifying a wavepacket initially situated at the level of a steady background flow with flow profile $\bar{u} = -u_{\rm DF}(z, t = 0)$. In these simulations, as time progresses and the wave moves vertically away from its initial position, the steady background flow is revealed about the initial position of the wavepacket while the opposite signed transient flow is observed to translate vertically with the wavepacket which, neglecting dispersion, is given by $\overline{u}_{\rm DF} \equiv (1/2)N|\vec{k}||A_0(\tilde{z})|^2$, with $\tilde{z} = z - c_{gz}t$.

For horizontally and vertically localized wavepackets, it is not appropriate to superimpose upon the wave field the divergent-flux induced flow $u_{\rm DF}$, because this is a divergent flow. Instead of making assumptions about the divergent-flux and response flow a priori, here we initialize with no wave-induced flow whatsoever and observe how the induced flow evolves as the wavepacket propagates. We will see that for both horizontally periodic and horizontally localized wavepackets, the horizontal velocity field evolves so that there is a horizontally integrated horizontal flow that translates with the wavepacket while a nearly equal and opposite but non-translating flow appears about the initial vertical location of the wavepacket.

B. Horizontally periodic wavepacket simulation

First, a simulation with a horizontally periodic wavepacket is performed with zero initial mean horizontal flow. This provides a basis for comparison with horizontally localized wavepackets. The results are shown in Figure 3 (Multimedia view). The initial condition in Figure 3(a) shows contours of the horizontal velocity field to the left and to the right shows the vertical profile of the horizontally integrated horizontal flow:

$$I_u \equiv \int_{-L_x}^{L_x} u \, dx, \tag{59}$$

in which the horizontal extent of the domain is the horizontal wavelength: $\lambda_x = 2L_x$. Because the wavepacket is horizontally periodic and we have not superimposed a mean background flow initially, $I_u(z, t = 0) = 0$ for all z.

At later times, the wavepacket is seen to propagate upwards at the predicted vertical group speed, being centred around $z \simeq 70$ at time $Nt = 200$. During its propagation, the horizontally integrated flow develops into a "double-jet" profile. A negative jet centred around $z = 0$ is evident at $Nt = 100$ and remains centred there at $Nt = 200$. Meanwhile, a positive jet appears, being centred around $z = 35k_x^{-1}$ at $Nt = 100$ and around $z = 70k_x^{-1}$ at $Nt = 200$. At this last time, the lower positive jet conforms almost exactly to the predicted horizontally integrated divergent-flux induced flow, defined by (35). Explicitly, the dashed line shows

$$I_{u,\rm DF} = \lambda_x \left\{ \frac{1}{2} N|\vec{k}|A_0{}^2 \exp\left[-(z - c_{gz}t)^2/\sigma_z{}^2\right] \right\}. \tag{60}$$

This simple prediction assumes the wavepacket translates at the group velocity from its initial position at the origin and does not disperse. Indeed the small discrepancy between I_u and $I_{u,\rm DF}$ at $Nt = 200$ about $z = 70k_x^{-1}$ is the result of dispersion. If $I_{u,\rm DF}$ is computed using $|A(z, t)|^2$ rather than $|A(z - c_{gz}t, t = 0)|^2$, the curves exactly overlap about $z = 70k_x^{-1}$.

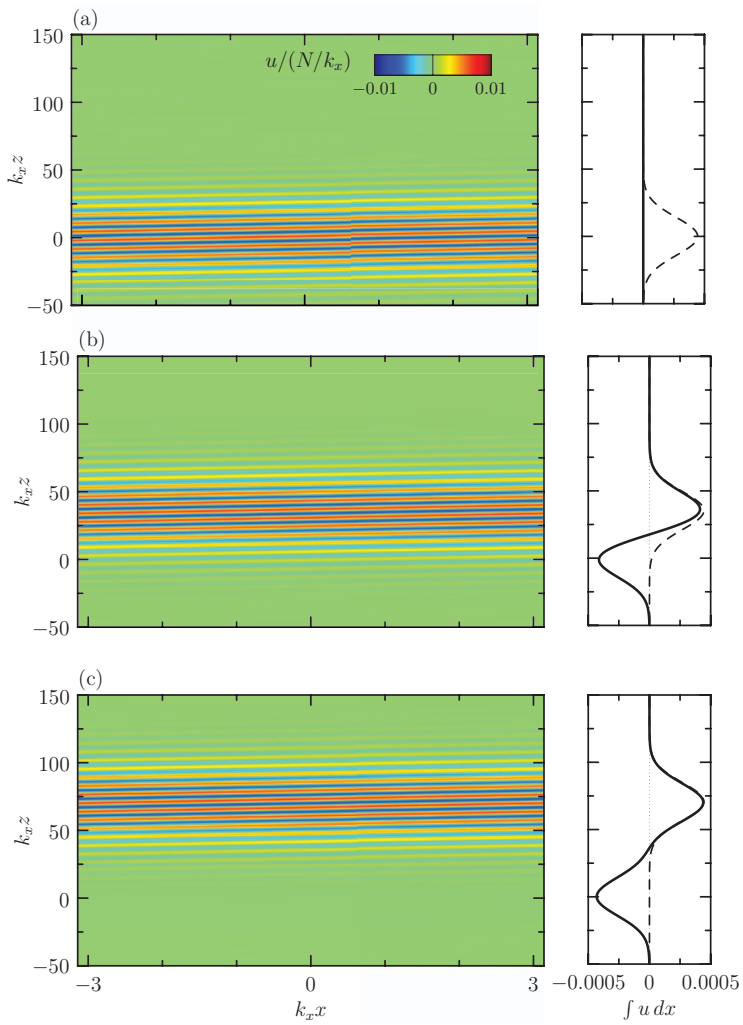

FIG. 3. Simulation of a horizontally periodic wavepacket at times $Nt =$ (a) 0, (b) 100, and (c) 200. The left panels show the horizontal velocity field, the right panels show the horizontally integrated horizontal flow I_u (black line). The dashed line plots the predicted integrated horizontal induced flow given by (60). (Multimedia view) [URL: http://dx.doi.org/10.1063/1.4899262.1] [URL: http://dx.doi.org/10.1063/1.4899262.2]

Momentum conservation for a Boussinesq fluid predicts that the domain integrated horizontal flow $\int I_u\,dz$ is unchanging in time. In our simulations, we indeed find that $\int I_u\,dz = 0$ at each time step. In particular, at $Nt = 200$ the positive momentum associated with the lower positive jet is exactly cancelled by the upper negative jet situated around $z = 0$. This result reaffirms the assertion by Sutherland[6] that simulations of horizontally periodic, vertically localized wavepackets in otherwise stationary fluid should nonetheless have a non-zero mean flow, $\bar{u}(z, t = 0) = u_{\mathrm{DF}}$, imposed at the outset. To require zero mean flow, as we have done in the simulation shown in Figure 3, means that one is actually simulating a wavepacket centred about a (steady) background negative jet whose speed is equal and opposite to the (transient) divergent-flux induced flow so that the sum of both equals zero at each height z. When the wavepacket propagates vertically away, the wave-induced flow moves with the waves and reveals itself as a positive, through vertically translating horizontal jet. Simultaneously the steady negative background jet is revealed.

Herein, the primary purpose of Figure 3 is to demonstrate that the wave-induced flow has fully separated from the background flow at $Nt = 200$. And so at this time, in a frame of reference moving at the group velocity the wavepacket and its induced flow can be regarded as being in steady state.

C. Horizontally localized wavepacket: Non-local wave-induced flow

We now consider the simulation of a horizontally as well as vertically localized wavepacket. Diagnostics at $Nt = 200$ are shown in Figure 4 (Multimedia view). This is the time at which the horizontally periodic wavepacket and its induced mean flow was shown to have reached steady state in a reference frame translating vertically at speed c_{gz}. Although the domain extended over $-3200 < k_x x < 3200$, here the fields are plotted only for $-100 \leq k_x x \leq 100$.

As expected, the horizontal and vertical velocity fields in Figures 4(a) and 4(b) show that the wavepacket has translated to the origin with little dispersion. Because the magnitude of the wave-induced flows is predicted to be of order amplitude squared, the signal is too weak to be seen on the colour scale shown in these two plots. Indeed, (41) predicts the magnitude of the induced horizontal flow to be $A_{0ur}/(N/k_x) \sim (\pi^{5/2}/128) \times 10^{-5} \simeq 1.4 \times 10^{-6}$.

To reveal the induced flows, we perform a horizontal fast Fourier transform of both fields over the entire domain and set to zero all Fourier components with horizontal wavenumbers between $0.5k_x$ and $1.5k_x$. Inverse transforming gives the resulting wavepacket-filtered horizontal and vertical velocity fields $\overline{u}$ and $\overline{w}$ shown in Figures 4(c) and 4(d), respectively. These fields, plotted with a colour scale spanning a much smaller range of non-dimensional speeds, e.g., $||\overline{u}|| < 2 \times 10^{-6} N/k_x$, show that magnitude of the horizontal response flow is indeed well-predicted by (41).

Even though the momentum flux divergence associated with the wavepacket is predicted to generate a local u and w-dependent divergent-flux induced flow according to (23), consistent with (34) the response flow results in a total wave-induced flow moving the fluid almost entirely in the x-direction. In Figure 4(c), $\overline{u}$ appears to be nearly independent of x. However, the plots of $\overline{u}$ over the entire horizontal computational domain in Figure 5 (Multimedia view) shows that $\overline{u}$ exhibits a pattern similar to a bow wake. Somewhat more directly, it resembles the pattern of internal waves created by a translating cylinder,[23,24] although in the case of a vertically translating cylinder the horizontal flow field is an odd function in x centred about the cylinder and in our case it is an even function of x centred about the wavepacket.

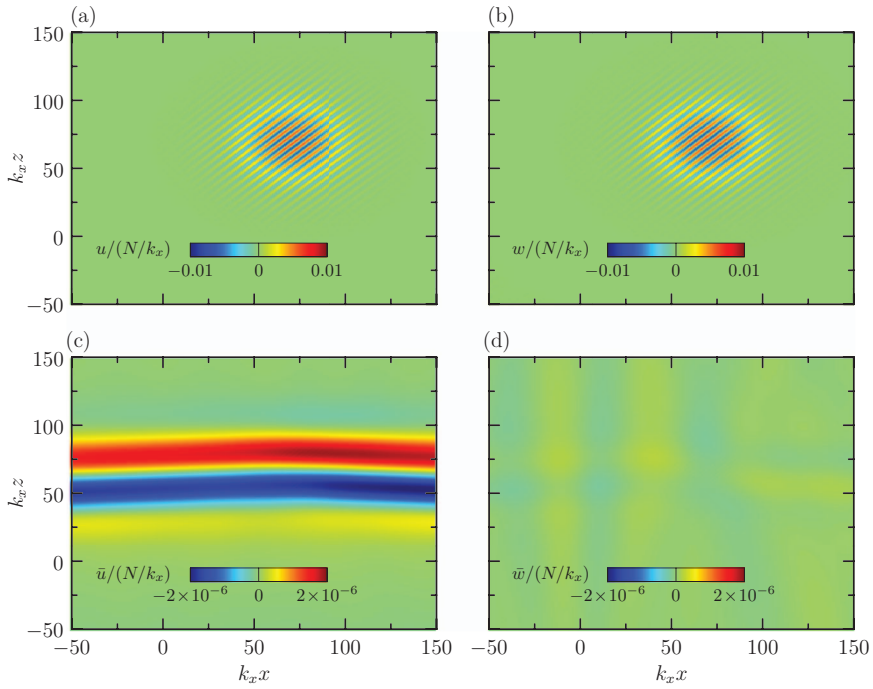

FIG. 4. Horizontally and vertically localized Gaussian wavepacket at $Nt = 200$ showing the (a) horizontal, u, and (b) vertical, w, velocity fields and the wavepacket-filtered (c) horizontal, u, and (d) vertical, w, velocity fields. (Multimedia view) [URL: http://dx.doi.org/10.1063/1.4899262.3]

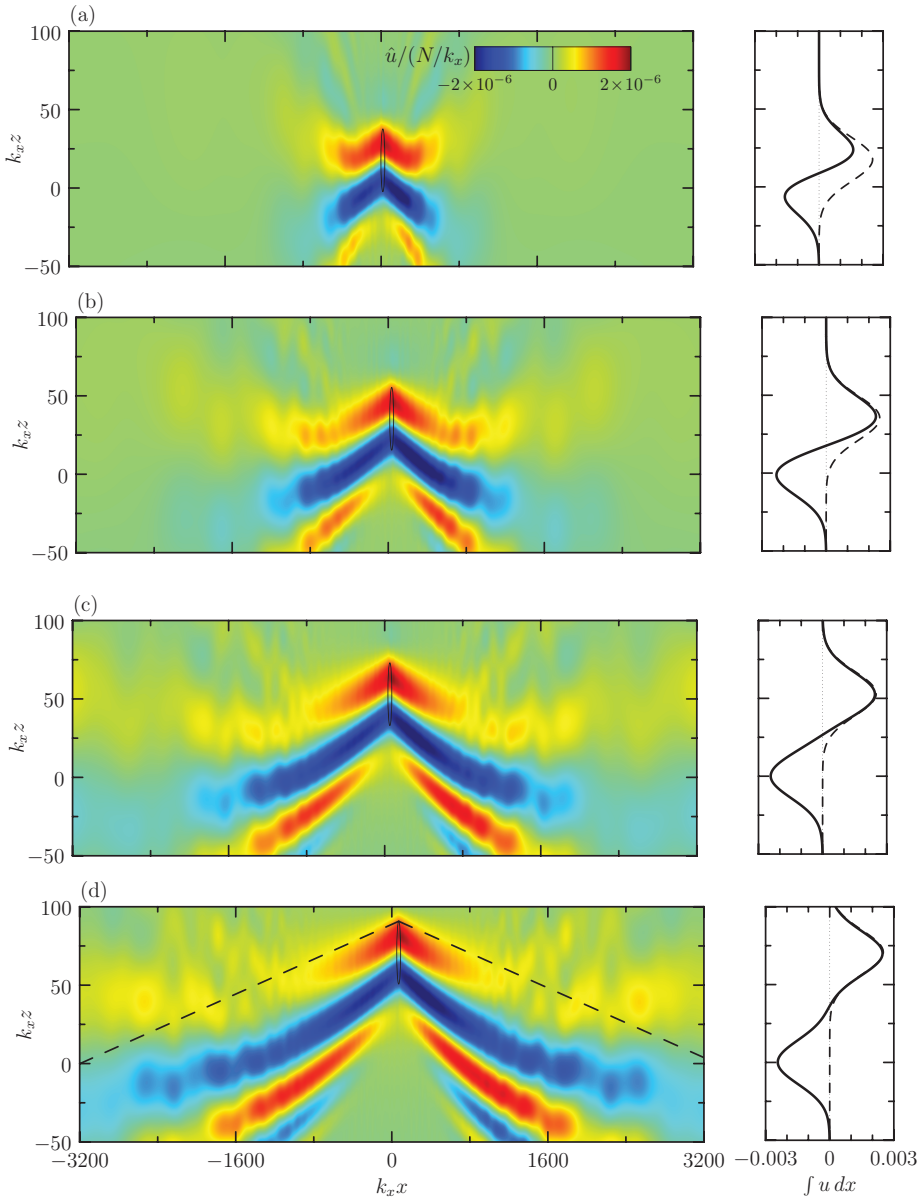

FIG. 5. Wavepacket-filtered horizontal flow (left) associated with the Gaussian wavepacket at Nt = (a) 50, (b) 100, (c) 150, and (d) 200 shown over the entire horizontal extent of the domain. The size of the localized wavepacket is indicted by the ellipse in each of the left-hand images. The diagonal dashed lines in the left-hand image of (d) are drawn with the slope of the long wave phase lines predicted by (39). The horizontally integrated horizontal velocity computed from the unfiltered horizontal velocity field is plotted by the solid lines in the corresponding panels to the right. The dashed line shows the prediction (61) for the horizontally integrated induced horizontal flow. (Multimedia view) [URL: http://dx.doi.org/10.1063/1.4899262.4] [URL: http://dx.doi.org/10.1063/1.4899262.5]

The result in Figure 4(c) clearly shows that the momentum flux divergence associated with the wavepacket acts as translating localized forcing that excites horizontally long internal waves. The slope of the phase-lines associated with these waves is consistent with the assumptions leading to the order-of-magnitude prediction (38) for the lateral extent of the wave-induced flow. The vertical wavelength of the long waves is on the order $\sigma_z = 20k_x^{-1}$ and the slope of the constant-phase lines predicted by (39) to have magnitude $|k_{xr}/k_{zr}| = \pi\epsilon_z/4\sqrt{2} \simeq 0.028$ is consistent with the slope evident in Figure 5(d).

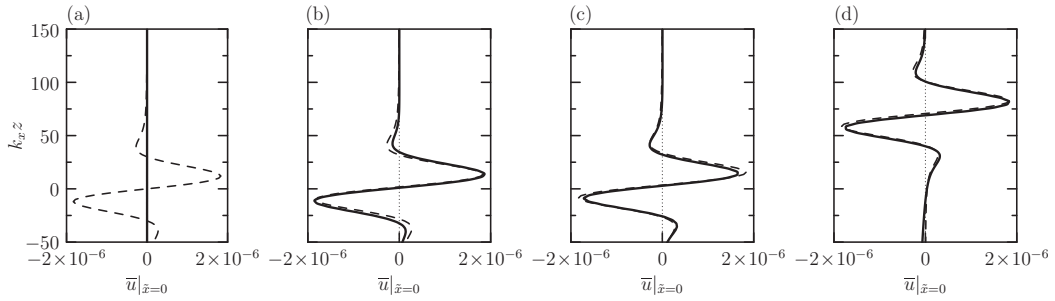

FIG. 6. Vertical profiles of the measured horizontal velocity (solid lines) at $\tilde{x} = 0$, corresponding to the horizontal position of the centre of the wavepacket, shown at nondimensional times $Nt =$ (a) 0, (b) 5, (c) 10, and (d) 200. These are compared with the predicted horizontal flow (dashed lines) given by (54).

Tracking the constant phase line of the long wave emanating from the front of the wavepacket at time $Nt = 200$ (Figure 5(d)), we see that the disturbance field becomes negligibly small at a vertical level corresponding to the trailing edge of the wavepacket. The lateral extent of the disturbance is $k_x|x| \simeq 1000$, close to the value $k_x L_i \simeq 1440 {k_x}^{-1}$ predicted by (38). The disturbance field further in the lee of the wavepacket continues to emanate outward. Yet this can be understood as the passive propagation of long waves after their forcing is turned off.

The long waves are the result of the wave-induced flow associated with the localized wavepacket. Despite the somewhat complex structure of the long waves, horizontally integrating the (unfiltered) horizontal velocity field reveals horizontal vertical profiles shown in the right panels of Figure 5 similar to those produced by a horizontally periodic wavepacket. Again, as time progresses, the initially zero flow evolves to reveal a superposition of a steady negative "jet" centred around $z = 0$ and a vertically translating positive "jet." (We have put the word "jet" in quotations here because the flow is in fact x-dependent, though over long horizontal distances compared with the wavepacket width.) Furthermore, the vertical structure of the "jet" is well predicted by theory. From (17) and (35), we predict

$$I_{u,\mathrm{DF}} = \sqrt{\pi}\sigma_x \left\{ \frac{1}{2} N |\vec{k}| {A_0}^2 \exp\left[-(z - c_{gz}t)^2 / {\sigma_z}^2 \right] \right\}. \tag{61}$$

The right-hand panels in Figure 5 show that this prediction closely overlaps with the integrated horizontal flow calculated from the simulations in the vicinity of the wavepacket after it has translated sufficiently far from its initial position and left the negative "jet" in its wake. Although the wave-induced velocities from momentum flux divergence (23) are of order $\alpha^2\epsilon^0$, the resulting velocities associated with the long wave corresponding to (61) are of order $\alpha^2\epsilon^1$, as shown in (41) setting $\epsilon = \epsilon_x = \epsilon_z$.

Comparing the structure of the predicted horizontal velocity shown in Fig. 2(b) (for a wavepacket centred at the origin) with the numerically computed horizontal velocity associated with the induced long wave shown in Fig. 5(d), it is clear that a wavepacket in an otherwise stationary ambient induces a long wave with the structure and amplitude predicted by theory.

While the horizontally integrated horizontal flow is positive over the vertical extent of the wavepacket, the induced horizontal flow measured along a vertical profile through the centre of the wavepacket changes from positive on the leading flank to negative on the trailing flank as illustrated in Figure 6. This shows vertical profiles of $\overline{u}(\tilde{x} = 0, z)$ at four different times and compares the results with the theoretical prediction given by (54). Because the ambient is stationary at $Nt = 0$, the measured wavepacket-filtered horizontal flow is zero at this time. However, after less than one buoyancy period the vertical profile of the wavepacket-filtered horizontal flow through the centre of the wavepacket conforms closely to the predicted flow (Figure 6(b)). The measurements and prediction are close to overlapping at $Nt = 10$ (Figure 6(c)) and much later at $Nt = 200$ (Figure 6(d)). This shows that a wavepacket generated in an ambient initially at rest rapidly induces a horizontal flow field across its breath whose structure can be predicted by steady-state theory.

V. CONCLUSIONS

We have examined theoretically and numerically the structure of the flow induced by a small-amplitude, two-dimensional, Boussinesq, horizontally and vertically localized internal gravity wavepacket. This induced flow is not the result of wave-breaking, but is a transient flow that varies broadly in space — compared to the width of the wavepacket — and which is coupled with the wavepacket as it moves at its group velocity.

Through a theoretical wavepacket approach that seeks a steady wave-induced flow in a frame of reference that moves with the group velocity of the wavepacket, we find that the leading-order total wave-induced horizontal flow is a horizontally uniform flow whose horizontal integral is equal to the horizontal integral of the horizontal component of the divergent-flux induced flow for internal waves u_{DF}.

Simulations show that an internal wavepacket indeed excites a long horizontal disturbance. But in a sufficiently wide horizontal domain, it is clear that the disturbance field is not horizontally uniform to the far reaches of the domain. In an incompressible fluid, information about the presence of the wavepacket can only be transmitted laterally at the speed of horizontally long internal waves. The structure and extent of the long disturbance was anticipated by Bretherton.[1] However, our analyses, combined with numerical simulations, clearly show that the wavepacket excites a long internal wave. Furthermore, our analyses reveal the link between the momentum transport by the wavepacket and the long wave. Consistent with theory, we find that the horizontally integrated horizontal flow associated with the long waves is well represented by the horizontal integral of u_{DF}. This result and the requirement that the horizontally long internal waves propagate with vertical phase speed equal to the vertical group velocity of the internal wavepacket gives a prediction, not just for the wavenumber, but also the amplitude of the long waves. Crucially, the characteristic horizontal scale of the induced long wave is much larger than the horizontal scale associated with the packet itself: the response is non-local.

This study has focused upon small-amplitude, Boussinesq internal wavepackets confined to two dimensions. If the spanwise extent of the wavepacket is finite, adding a third dimension to the problem, then it is possible for a component of the response flow to circulate laterally around the wavepacket in what has been called "Bretherton flow" (e.g., see Figure 3(a) of Bühler and McIntyre).[9] There is some recent experimental evidence for a recirculating flow resulting from a spanwise localized internal wave beam,[25] though viscosity played an important role in that study. The dynamics are expected to be more complicated if the waves are large-amplitude or grow to large amplitude through non-Boussinesq effects.[7,17,19] Horizontally periodic, vertically localized internal wavepackets have been shown to be modulationally unstable if their frequency is larger than that for waves with the fastest vertical group velocity. The amplitude-envelope of these waves narrows and grows and advances vertically at a slower speed as a consequence of being Doppler-shifted by the wave-induced mean flow. Otherwise the waves are modulationally stable and the wavepacket broadens vertically. Qualitatively, the same weakly nonlinear dynamics have been observed for wavepackets that are horizontally as well as vertically localized.[17] This can now be understood to occur due to weakly nonlinear interactions between the wavepacket and the horizontal flow associated with the induced long wave. Weakly nonlinear theory has also provided evidence for radiating wave-like disturbances excited by moderately large, fully three-dimensional wavepackets.[26] But more needs to be done by way of theory and high resolution simulations in large computational domains. Future work will investigate weakly nonlinear effects associated with interactions between a spanwise-finite, large-amplitude internal wavepackets and the induced long wave it generates. The ultimate goal is to evaluate the transport of momentum and energy, not only by the wavepacket, but by the horizontally long internal waves they generate.

ACKNOWLEDGMENTS

The authors are grateful for insights provided by Oliver Bühler. This research was in part supported by the National Science Foundation (Grant No. OCE- 0824636) and the Office of Naval Research (Grant No. N00014-09-1-0844) through their support of the 2013 WHOI Geophysical Fluid Dynamics Summer School where the work presented here was first undertaken.

APPENDIX: NONLINEAR FORCING OF LONG INTERNAL WAVES

Here we compute the leading-order non-zero expression for $\nabla \cdot \vec{F}$ in (30), in which $\vec{F}$ is given explicitly by

$$\vec{F} \equiv \Big[\frac{\partial}{\partial t}\big[\zeta^{(1)}\,\vec{u}^{(1)}\big] + N^2\frac{\partial}{\partial x}\big[\xi^{(1)}\,\vec{u}^{(1)}\big]\Big], \tag{A1}$$

and the velocity, vorticity, and vertical displacement fields $\vec{u}^{(1)}$, $\zeta^{(1)}$, and $\xi^{(1)}$ are given in terms of the quasi-monochromatic internal wavepacket. Further to (19), we neglect dispersion, expressed through the dependence of the amplitude envelope upon the slow variable T. Thus for the vertical displacement field we suppose at leading order:

$$\xi^{(1)} = \xi_0^{(1)} \equiv A(X, Z)e^{\imath\varphi}, \tag{A2}$$

in which it is understood that the actual field is the real part of the right-hand side, $\varphi \equiv k_x x + k_z z - \omega t$, and $(X, Z) = (\epsilon(x - c_{gx}t), \epsilon(z - c_{gz}t))$ represent the slow spatial variables associated with the amplitude envelope that translates at the group velocity of the wavepacket. Here we have assumed the slow vertical and horizontal scales are comparable in magnitude so that $\epsilon \equiv \epsilon_x = \epsilon_z$. For convenience here, we also drop the superscript, (1), with the understanding that all the fields under consideration are $O(\alpha)$ and so write the perturbation expansion in ϵ for each of the fields as $\zeta = \zeta_0 + \epsilon\zeta_1 + \ldots$, etc.

From the linearized equations of motion for internal waves, we express the $O(\epsilon^0)$ fields in terms of the vertical displacement amplitude envelope, as listed in the second column of Table I. At $O(\epsilon)$, we assume that ξ is an imposed field and so set $\xi_1^{(1)} \equiv 0$ (and $\xi_n^{(1)} \equiv 0$ for $n \geq 1$). To get the remaining fields we extract terms involving exactly one derivative of the amplitude envelope. So, for example, from the differential relations $w = \partial_t\xi = \partial_x\psi$ we find

$$-c_{gx}A_X e^{\imath\varphi} - c_{gz}A_Z e^{\imath\varphi} = -(N/|\vec{k}|)A_X e^{\imath\varphi} + \imath k_x\psi_1,$$

in which the subscripts to A denote partial derivatives. Solving for ψ_1 and simplifying using $c_{gx} = Nk_z^2/|\vec{k}|^3$ and $c_{gz} = -Nk_xk_z/|\vec{k}|^3$ gives

$$\psi_1 = -\imath(N/|\vec{k}|^3)[k_xA_X + k_zA_Z]e^{\imath\varphi}.$$

This and the corresponding expressions for the other $O(\epsilon)$ fields of interest are given in the third column of Table I.

Next, we consider the leading-order, $O(\alpha^2\epsilon^1)$, contributions from each of the four products of pairs of fields in the expression for $\vec{F}$ in (A1). In doing so, we explicitly extract the real part of each expression and keep only the slowly varying result (i.e., those terms in the product for which $e^{\imath\varphi}$ multiplies its complex conjugate). At $O(\alpha^2\epsilon^0)$ the result gives zero. At next order in ϵ we consider

TABLE I. Expressions for different fields at $O(\alpha\epsilon^0)$ (second column) and $O(\alpha\epsilon^1)$ (third column) given in terms of the amplitude envelope A of the vertical displacement field, as found through the linearized equations for internal waves. It is understood that the actual fields are the real parts of the tabulated expressions.

Field	$O(\epsilon^0)$	$O(\epsilon^1)$
Vertical displacement	$\xi_0 = Ae^{\imath\varphi}$	$\xi_1 = 0$
Streamfunction	$\psi_0 = -(N/\|\vec{k}\|)Ae^{\imath\varphi}$	$\psi_1 = -\imath(N/\|\vec{k}\|^3)[k_xA_X + k_zA_Z]e^{\imath\varphi}$
Horizontal velocity	$u_0 = \imath(Nk_z/\|\vec{k}\|)Ae^{\imath\varphi}$	$u_1 = (Nk_x/\|\vec{k}\|^3)[-k_zA_X + k_xA_Z]e^{\imath\varphi}$
Vertical velocity	$w_0 = -\imath(Nk_x/\|\vec{k}\|)Ae^{\imath\varphi}$	$w_1 = (Nk_z/\|\vec{k}\|^3)[-k_zA_X + k_xA_Z]e^{\imath\varphi}$
Vorticity	$\zeta_0 = -N\|\vec{k}\|Ae^{\imath\varphi}$	$\zeta_1 = \imath(N/\|\vec{k}\|)[k_xA_X + k_zA_Z]e^{\imath\varphi}$

the product of $O(\epsilon^0)$ fields with $O(\epsilon^1)$ fields. Thus we find the following:

$$\begin{aligned}
(\overline{\zeta u})_1^{(2)} &= \frac{\epsilon}{4}(N^2/|\vec{k}|^2)\left[2k_xk_z\partial_X + (k_z^2 - k_x^2)\partial_Z\right]|A|^2,\\
(\overline{\zeta w})_1^{(2)} &= \frac{\epsilon}{4}(N^2/|\vec{k}|^2)\left[(k_z^2 - k_x^2)\partial_X - (2k_xk_z)\partial_Z\right]|A|^2,\\
(\overline{\xi u})_1^{(2)} &= \frac{\epsilon}{4}(Nk_x/|\vec{k}|^3)\left[-k_z\partial_X + k_x\partial_Z\right]|A|^2,\\
(\overline{\xi w})_1^{(2)} &= \frac{\epsilon}{4}(Nk_z/|\vec{k}|^3)\left[-k_z\partial_X + k_x\partial_Z\right]|A|^2.
\end{aligned} \tag{A3}$$

These expressions may be substituted into (A1) to get the nonlinear forcing at $O(\alpha^2\epsilon^3)$. After some simplifying we find

$$\begin{aligned}
(\nabla\cdot\vec{F})_3^{(2)} = \frac{1}{4}\epsilon^3\frac{N^3}{|\vec{k}|^5}\Big[&- k_xk_z(3k_z^3 + k_x^2)\,\partial_{XXX} + (k_z^4 + 4k_z^2k_x^2 + k_x^4)\,\partial_{XXZ}\\
&+ k_xk_z(5k_z^2 - k_x^2)\,\partial_{XZZ} - 2k_x^2k_z^2\,\partial_{ZZZ}\Big]|A|^2.
\end{aligned} \tag{A4}$$

[1] F. P. Bretherton, "On the mean motion induced by gravity waves," J. Fluid Mech. **36**, 785–803 (1969).
[2] T. N. Palmer, G. J. Shutts, and R. Swinbank, "Alleviation of a systematic westerly bias in general circulation and numerical weather prediction models through an orographic gravity drag parametrization," Q. J. R. Meteorol. Soc. **112**, 1001–1039 (1986).
[3] N. A. McFarlane, "The effect of orographically excited gravity wave drag on the general circulation of the lower stratosphere and troposphere," J. Atmos. Sci. **44**, 1775–1800 (1987).
[4] C. McLandress, "On the importance of gravity waves in the middle atmosphere and their parameterization in general circulation models," J. Atmos. Sol.-Terr. Phys. **60**, 1357–1383 (1998).
[5] R. S. Lindzen, "Turbulence and stress owing to gravity wave and tidal breakdown," J. Geophys. Res. **86**, 9707–9714, doi:10.1029/JC086iC10p09707 (1981).
[6] B. R. Sutherland, "Weakly nonlinear internal wavepackets," J. Fluid Mech. **569**, 249–258 (2006).
[7] H. V. Dosser and B. R. Sutherland, "Anelastic internal wavepacket evolution and stability," J. Atmos. Sci. **68**, 2844–2859 (2011).
[8] F. Rieper, U. Achatz, and R. Klein, "Range of validity of an extended WKB theory for atmospheric gravity waves: One-dimensional and two-dimensional case," J. Fluid Mech. **729**, 330–363 (2013).
[9] O. Bühler and M. E. McIntyre, "Wave capture and wave-vortex duality," J. Fluid Mech. **534**, 67–95 (2005).
[10] O. Bühler, *Waves and Mean Flows* (Cambridge University Press, Cambridge, UK, 2009) p. 341.
[11] G. G. Stokes, "On the theory of oscillatory waves," Trans. Cambridge Philos. Soc. **8**, 441–455 (1847).
[12] M. Longuet-Higgins and R. Stewart, "Radiation stress and mass transport in gravity waves, with applications to "surf beats"," J. Fluid Mech. **13**, 481–504 (1962).
[13] M. E. McIntyre, "On the wave momentum myth," J. Fluid Mech. **106**, 331–347 (1981).
[14] F. P. Bretherton and C. J. R. Garrett, "Wavetrains in inhomogeneous moving media," Proc. R. Soc. London, Ser. A **302**, 529–554 (1969).
[15] D. J. Acheson, "On over-reflexion," J. Fluid Mech. **77**, 433–472 (1976).
[16] J. F. Scinocca and T. G. Shepherd, "Nonlinear wave-activity conservation laws and Hamiltonian structure for the two-dimensional anelastic equations" J. Atmos. Sci. **49**, 5–27 (1992).
[17] B. R. Sutherland, "Finite-amplitude internal wavepacket dispersion and breaking," J. Fluid Mech. **429**, 343–380 (2001).
[18] B. R. Sutherland, *Internal Gravity Waves* (Cambridge University Press, Cambridge, UK, 2010), p. 378.
[19] H. V. Dosser and B. R. Sutherland, "Weakly nonlinear non-Boussinesq internal gravity wavepackets," Physica D **240**, 346–356 (2011).
[20] V. P. Starr, "A momentum integral for surface waves in deep water," J. Mar. Res. **6**, 126–135 (1947).
[21] W. H. Press, S. A. Teukolsky, W. T. Vetterling, and B. P. Flannery, *Numerical Recipes: The Art of Scientific Computing*, 3rd ed. (Cambridge University Press, New York, USA, 2007), p. 1235.
[22] B. R. Sutherland and W. R. Peltier, "Turbulence transition and internal wave generation in density stratified jets," Phys. Fluids **6**, 1267–1284 (1994).
[23] T. N. Stevenson and N. H. Thomas, "Two-dimensional internal waves generated by a travelling oscillating cylinder," J. Fluid Mech. **36**, 505–511 (1969).
[24] B. Voisin, "Internal wave generation in uniformly stratified fluids. Part 2. moving point sources," J. Fluid Mech. **261**, 333–374 (1994).
[25] G. Bordes, A. Venaille, S. Joubaud, P. Odier, and T. Dauxois, "Experimental observation of a strong mean flow induced by internal gravity waves," Phys. Fluids **24**, 086602 (2012).
[26] A. Tabaei and T. R. Akylas, "Resonant long-short wave interactions in an unbounded rotating stratified fluid," Stud. Appl. Math. **119**, 271–296 (2007).